Electronic Supplementary Information

Experimental and theoretical understanding on electrochemical activation and inactivation processes of $Nb_3O_7(OH)$ for ambient electrosynthesis of NH_3

Tianxing Wu,[a,1] Miaomiao Han,[a,1] Xiaoguang Zhu,[a] Guozhong Wang,[a] Yunxia Zhang,[a] Haimin Zhang[a,*] and Huijun Zhao[a,b]

[a] Key Laboratory of Materials Physics, Centre for Environmental and Energy Nanomaterials, Anhui Key Laboratory of Nanomaterials and Nanotechnology, CAS Center for Excellence in Nanoscience, Institute of Solid State Physics, Chinese Academy of Sciences, Hefei, 230031 Anhui, PR China

[b] Centre for Clean Environment and Energy, Griffith University, Gold Coast Campus, QLD 4222, Australia

[1] These authors contributed equally to this work.

*E-mail: zhanghm@issp.ac.cn (Haimin Zhang)

Table S1. Comparison of the NRR activity of $Nb_3O_7(OH)$/CFC electrocatalyst with other aqueous-based catalysts reported recently under ambient conditions.

Catalyst	**Electrolyte**	**Potential (vs. RHE)**	**NH_3 yield rate**	**FE**	**Reference**
$Nb_3O_7(OH)$/CFC	**0.1 M Na_2SO_4**	**-0.4 V**	**622 μg mg^{-1} h^{-1}**	**39.9 %**	**This work**
Pd/C	0.1 M PBS	0.1 V	4.5 μg mg^{-1} h^{-1}	8.2 %	1
$Pd_{0.2}Cu_{0.8}$/rGO	0.1 M KOH	-0.2 V	2.8 μg mg^{-1} h^{-1}	-	2
AuHNCs	0.5 M $LiClO_4$	-0.4 V	2.3 μg cm^{-2} h^{-1}	30.2 %	3
AuSAs-NDPCs	0.1 M HCl	-0.2 V	2.32 μg cm^{-2} h^{-1}	12.3 %	4
Au	5 mM H_2SO_4	-0.1 V	1305 μg mg^{-1} h^{-1}	11.1 %	5
Ru SAs/N-C	0.05 M H_2SO_4	-0.2 V	120.9 μg mg^{-1} h^{-1}	29.6 %	6
Ru@NC	0.1 M HCl	-0.21 V	3665 μg mg^{-1} h^{-1}	7.5 %	7
MnO	0.1 M Na_2SO_4	-0.39 V	1.11×10^{-10} mol s^{-1} cm^{-2}	8.02 %	8
Mn_3O_4	0.1 M Na_2SO_4	-0.8 V	11.6 μg mg^{-1} h^{-1}	3.0 %	9
MoS_2	0.1 M Na_2SO_4	-0.5 V	8.08×10^{-11} mol s^{-1} cm^{-2}	1.17 %	10
defect-rich MoS_2	0.1 M Na_2SO_4	-0.4 V	29.28 μg mg^{-1} h^{-1}	8.34 %	11
C-doped TiO_2	0.1 M Na_2SO_4	-0.7 V	16.22 μg mg^{-1} h^{-1}	1.84 %	12

d-TiO_2/TM	0.1 M HCl	-0.15 V	1.24×10^{-10} mol s^{-1} cm^{-2}	9.17 %	13
SnO_2	0.1 M Na_2SO_4	-0.7 V	1.47×10^{-10} mol s^{-1} cm^{-2}	2.17 %	14
Nb_2O_5 nanofiber	0.1 M HCl	-0.55 V	43.6 μg mg^{-1} h^{-1}	9.26 %	15
Nb_2O_5 nanowire	0.1 M Na_2SO_4	-0.6 V	1.58×10^{-10} mol s^{-1} cm^{-2}	2.26 %	16
NbO_2	0.05 M H_2SO_4	-0.65 V	11.6 μg mg^{-1} h^{-1}	32 %	17
Cr_2O_3	0.1 M HCl	-0.75 V	28.13 μg mg^{-1} h^{-1}	8.56 %	18
Mo_2C/C	0.5 M $LiSO_4$	-0.3 V	11.3 μg mg^{-1} h^{-1}	7.8 %	19
CeO_2	0.1 M Na_2SO_4	-0.5 V	16.4 μg mg^{-1} h^{-1}	3.7 %	20
Y_2O_3	0.1 M Na_2SO_4	-0.9 V	1.06×10^{-10} mol s^{-1} cm^{-2}	2.53 %	21
S-doped carbon	0.1 M Na_2SO_4	-0.7 V	19.07 μg mg^{-1} h^{-1}	7.47 %	22
boron carbide	0.1 M HCl	-0.75 V	26.57 μg mg^{-1} h^{-1}	15.95 %	23
B-doped graphene	0.05 M H_2SO_4	-0.5 V	9.8 μg h^{-1} cm^{-2}	10.8 %	24
black phosphorus	0.01 M HCl	-0.7 V	31.37 μg mg^{-1} h^{-1}	3.09 %	25
polymeric carbon nitride	0.1 M HCl	-0.2 V	8.09 μg mg^{-1} h^{-1}	11.59 %	26

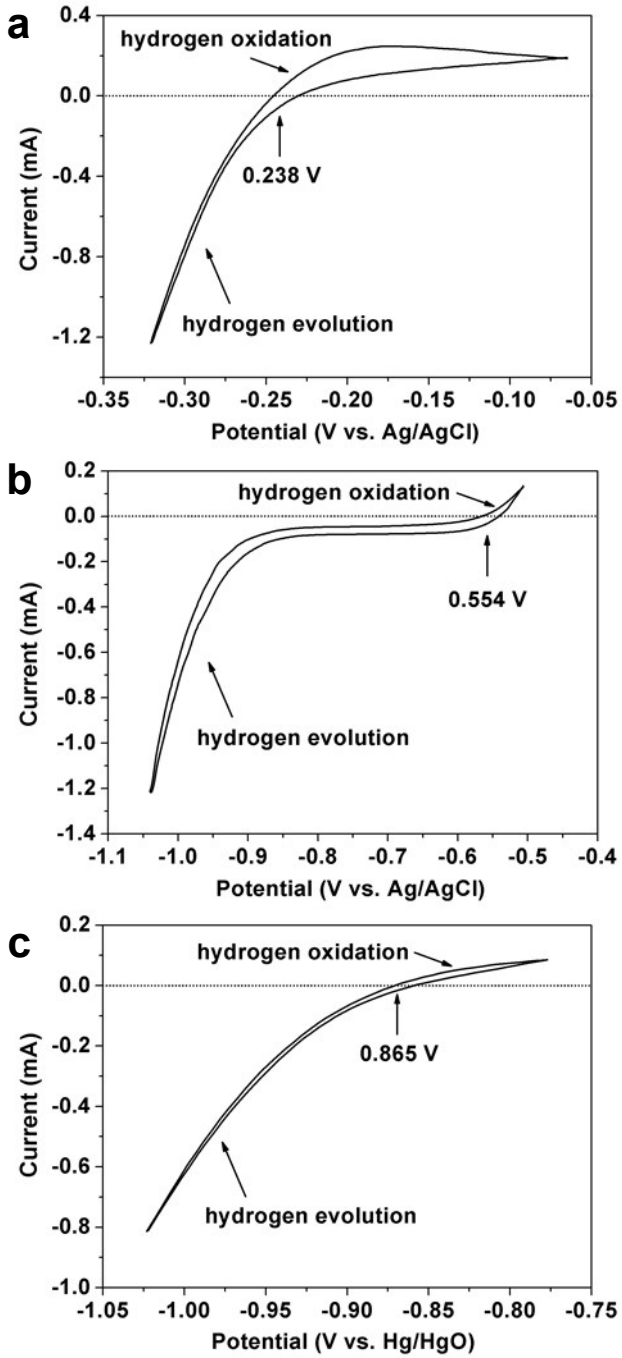

Fig. S1 CV curves of Pt sheet in different electrolytes with different reference electrodes at a scan rate of 1.0 mV s^{-1}. (a) H_2-saturated 0.1 M H_2SO_4 (Ag/AgCl as reference electrode), (b) H_2-saturated 0.1 M Na_2SO_4 (Ag/AgCl as reference electrode) and (c) H_2-saturated 0.1 M NaOH (Hg/HgO as reference electrode).

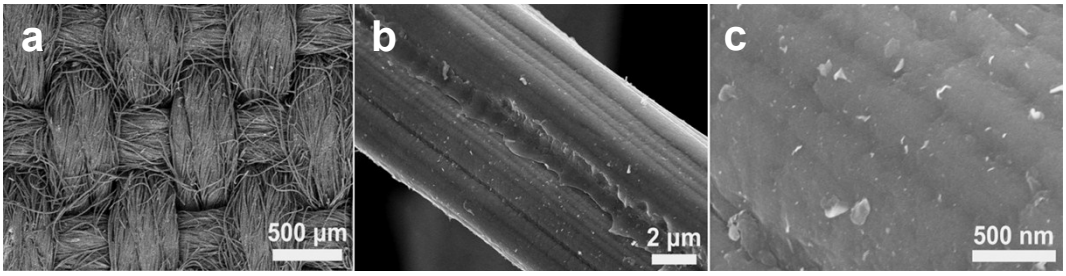

Fig. S2 Surface SEM images of commercial carbon fiber cloth (CFC). (a) Low-magnification SEM image; (b) SEM image of an individual carbon fiber; (c) High-magnification SEM image of an individual carbon fiber.

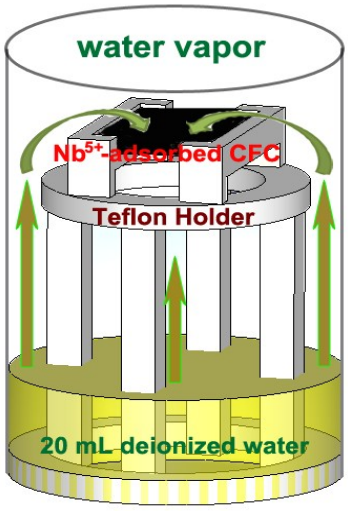

Fig. S3 Experimental set up of vapor-phase hydrothermal (VPH) method used in this work.

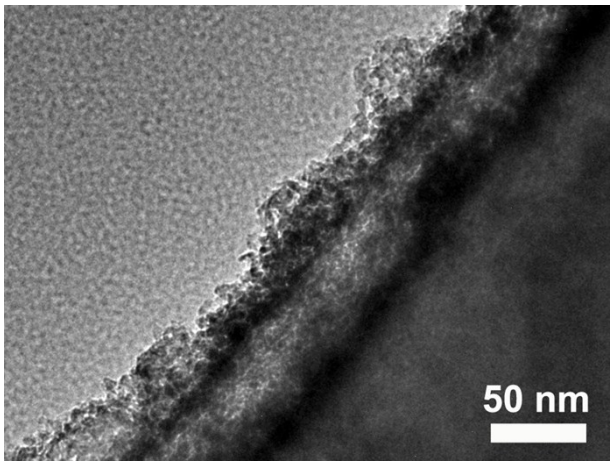

Fig. S4 TEM image of the $Nb_3O_7(OH)$/CFC without ultrathin slice treatment.

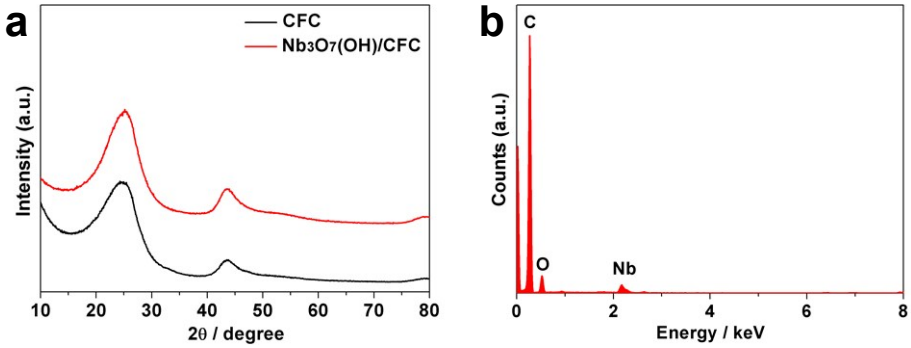

Fig. S5 (a) XRD patterns of pristine CFC and $Nb_3O_7(OH)$/CFC samples; (b) EDX spectrum of $Nb_3O_7(OH)$/CFC sample.

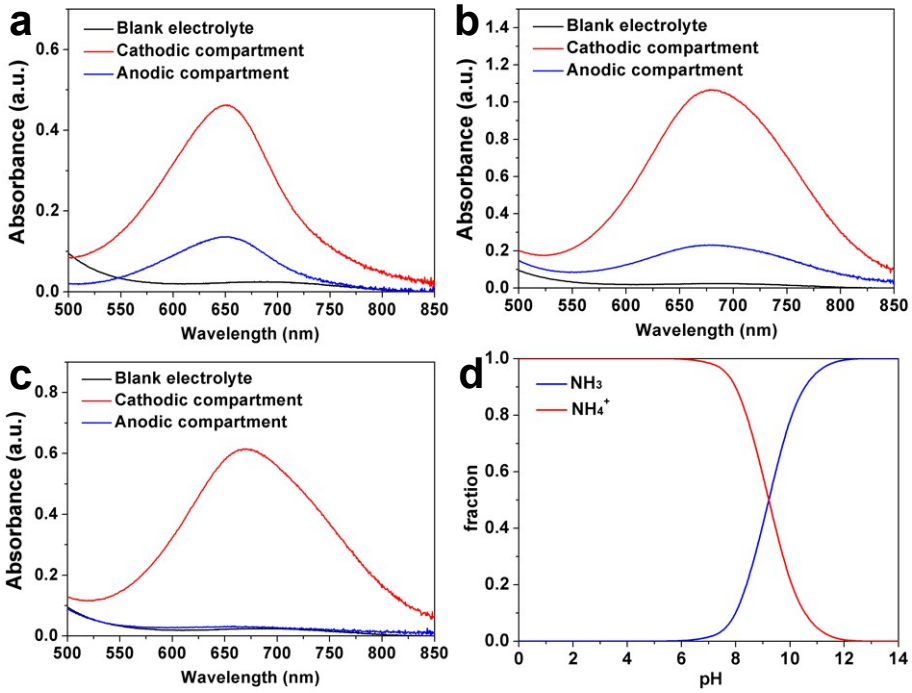

Fig. S6 The diffusion of NH_4^+ through the proton exchange membrane (Nafion 117) in three different electrolytes through an additional experiment approach. (a) 0.1 M H_2SO_4; (b) 0.1 M Na_2SO_4; (c) 0.1 M NaOH. In experiments, 2.0 mL of 10 ppm NH_4Cl solution was added to the cathodic compartment of H-type cell containing 20 mL of different electrolytes, then the electrolyte in both cathodic and anodic compartments was detected using the indophenol blue method after stirring for 30 min under an open system. (d) The distribution curves of NH_3 and NH_4^+ with different solution pHs.

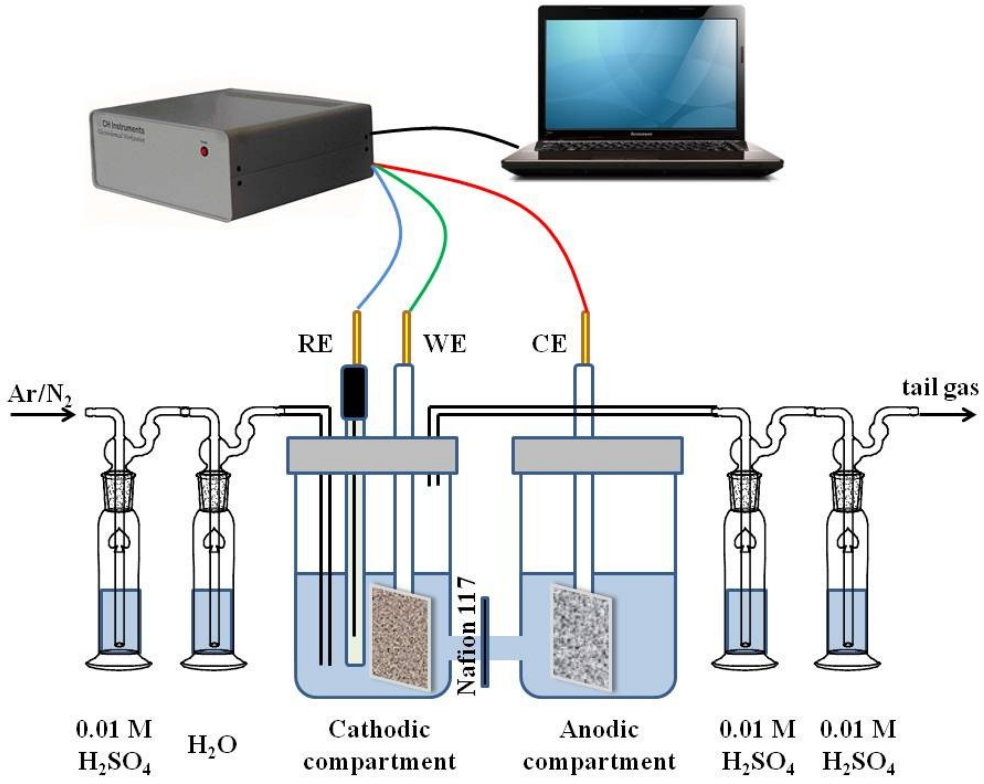

Fig. S7 Schematic diagram of two-compartment H-type electrochemical cell with three-electrode configuration and two-series tail gas absorbers (each absorber contains 20 mL of 0.01 M H_2SO_4 solution) to conduct the NRR measurements.

In experiments, the used Ar or N_2 was firstly purified by 0.01 M H_2SO_4 solution and distilled water to eliminate the possible interferences of NH_3 and NO_x in Ar or N_2. After NRR, the produced tail gas (*e.g.*, N_2) was further absorbed by two-series tail gas absorbers (each absorber contains 20 mL of 0.01 M H_2SO_4 solution) to prevent the produced NH_3 during NRR with N_2 flow into air. The produced NH_3 samples were subsequently collected from three parts of cathodic compartment, anodic compartment and tail gas absorber.

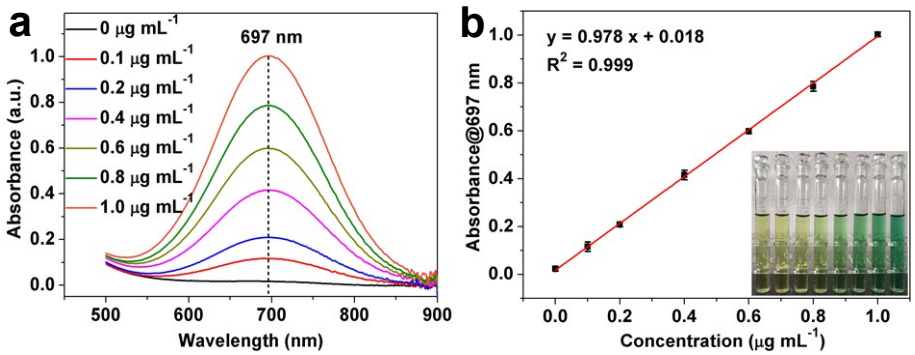

Fig. S8 (a) UV-Vis absorption spectra of various NH_4^+-N concentrations and (b) Corresponding calibration curves for the colorimetric NH_4^+-N assay using the indophenol blue method in 0.1 M Na_2SO_4 electrolyte. The error bars correspond to the standard deviations of multiple measurements.

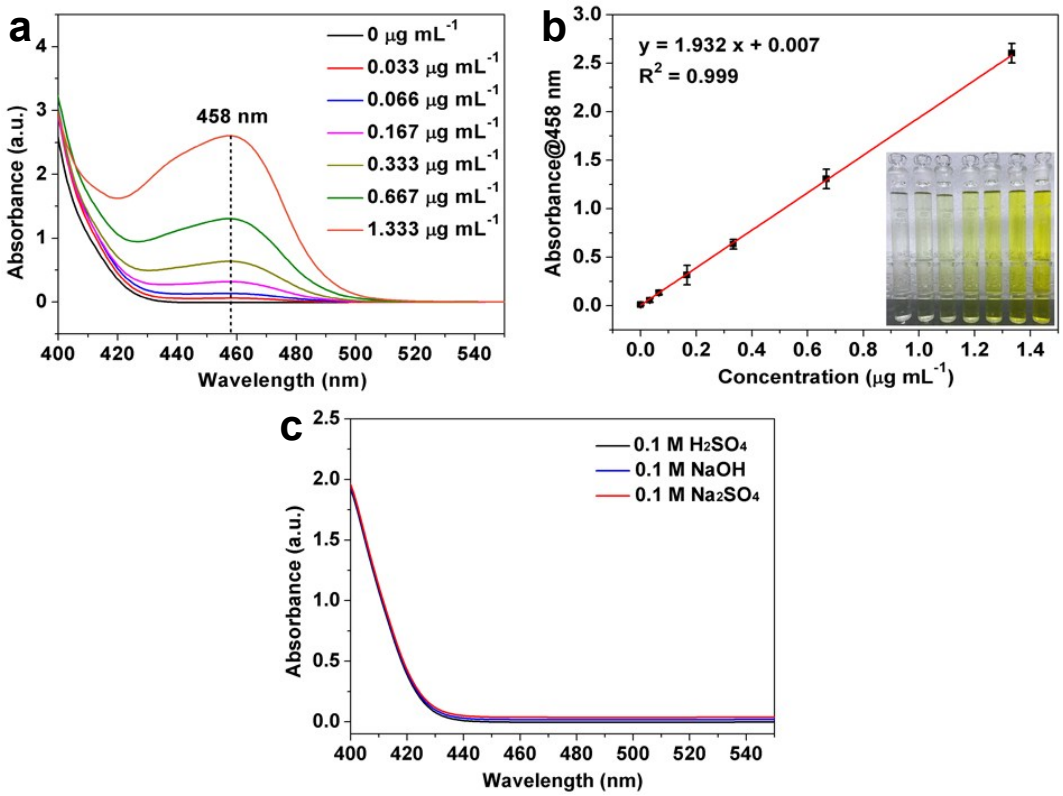

Fig. S9 (a) UV-Vis absorption spectra of various $N_2H_4 \cdot H_2O$ and (b) Corresponding calibration curves for the colorimetric $N_2H_4 \cdot H_2O$ assay using the Watt and Chrisp method in 0.1 M Na_2SO_4 electrolyte. The error bars correspond to the standard deviations of multiple measurements. (c) UV-Vis absorption spectra of different electrolytes (N_2-saturated 0.1 M H_2SO_4, 0.1 M NaOH and 0.1 M Na_2SO_4) after electrolysis at -0.4 V *vs.* RHE for 30 min.

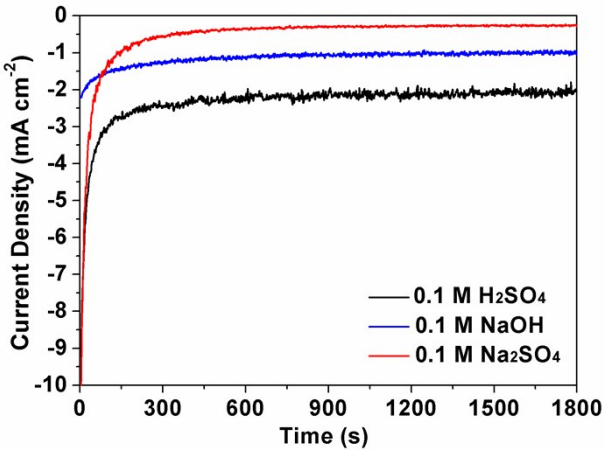

Fig. S10 Chronoamperometric curves of the $Nb_3O_7(OH)$/CFC measured in N_2-saturated 0.1 M H_2SO_4, 0.1 M NaOH and 0.1 M Na_2SO_4 electrolyte at -0.4 V *vs.* RHE for 30 min NRR.

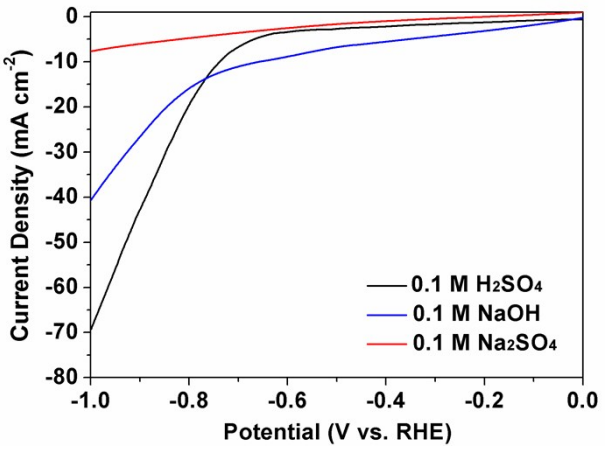

Fig. S11 LSV curves of the $Nb_3O_7(OH)$/CFC measured in Ar-saturated 0.1 M H_2SO_4, 0.1 M NaOH and 0.1 M Na_2SO_4 electrolytes with a scan rate of 5.0 mV s^{-1}.

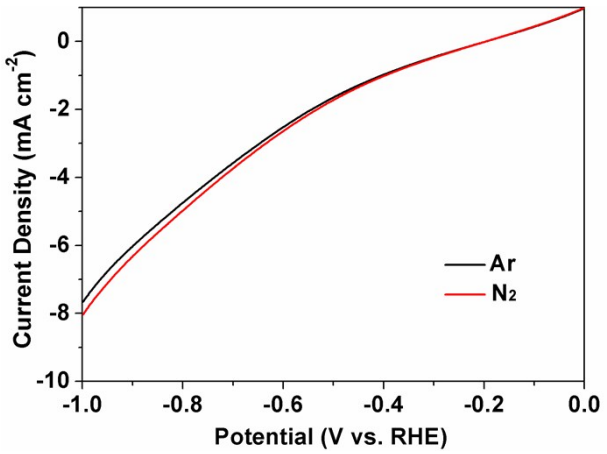

Fig. S12 LSV curves of THE $Nb_3O_7(OH)$/CFC in Ar- and N_2-saturated 0.1 M Na_2SO_4 electrolyte with a scan rate of 5.0 mV s^{-1}.

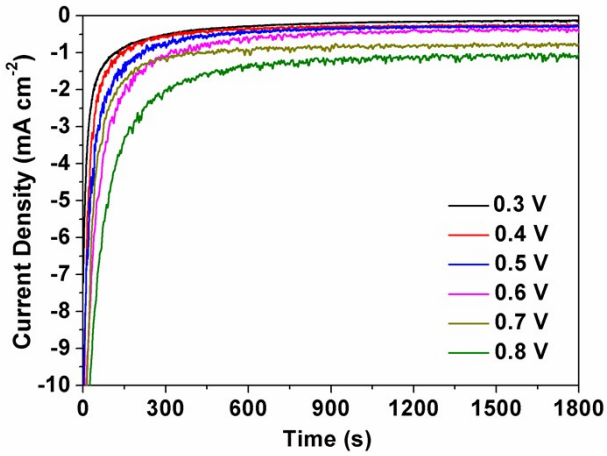

Fig. S13 Chronoamperometric curves of the $Nb_3O_7(OH)$/CFC measured in N_2-saturated 0.1 M Na_2SO_4 electrolyte under different potentials (*vs.* RHE).

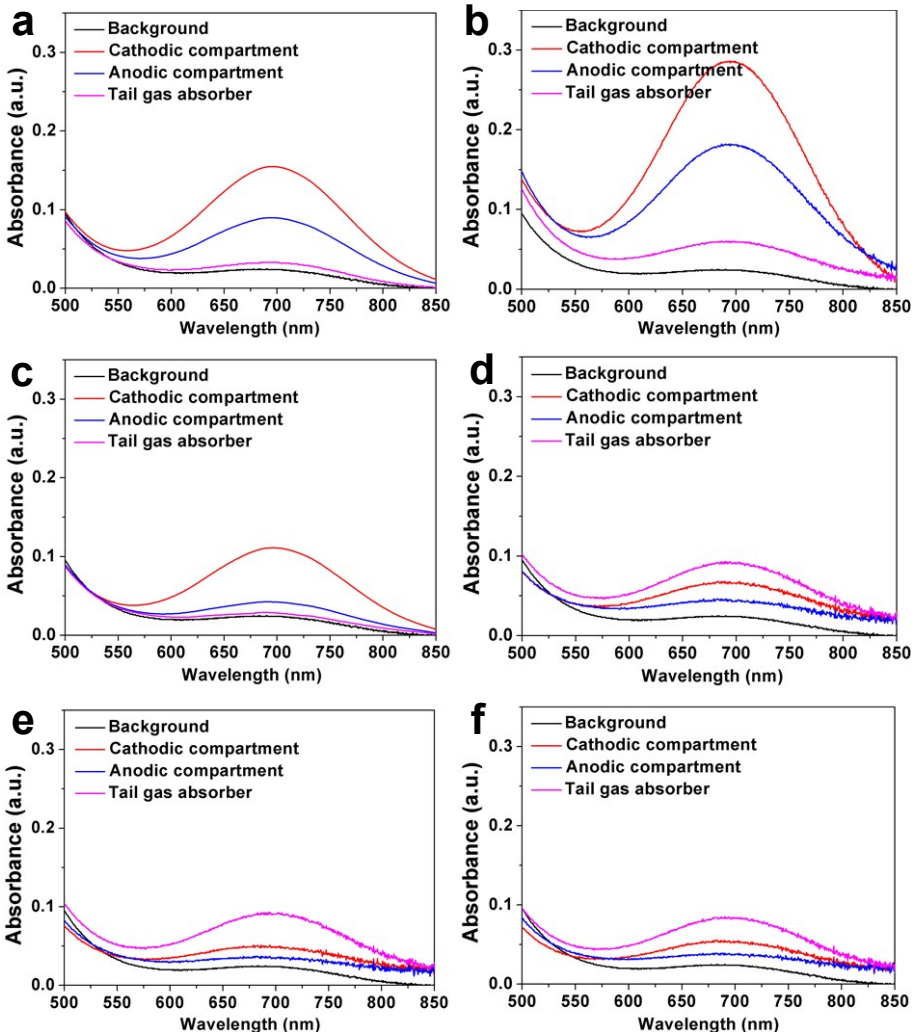

Fig. S14 UV-Vis absorption spectra of the collected samples from cathodic compartment, anodic compartment and tail gas absorber after NRR for 30 min in N_2-saturated 0.1 M Na_2SO_4 electrolyte at different potentials (*vs.* RHE) of (a) -0.3 V; (b) -0.4 V; (c) -0.5 V; (d) -0.6 V; (e) -0.7 V; (f) -0.8 V.

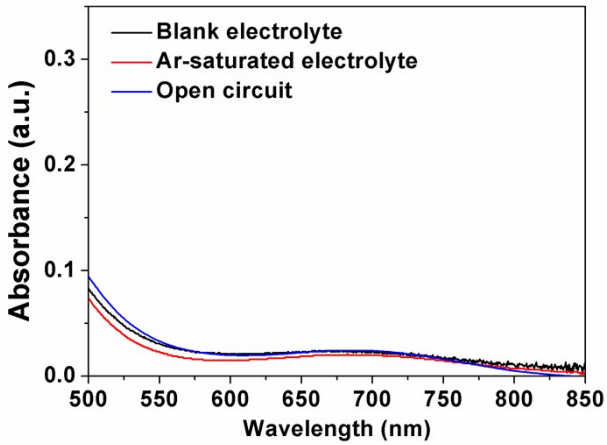

Fig. S15 UV-Vis absorption spectra of the electrolytes with different conditions: blank 0.1 M Na_2SO_4 electrolyte, Ar-saturated 0.1 M Na_2SO_4 electrolyte, and N_2-saturated 0.1 M Na_2SO_4 electrolyte at open circuit condition.

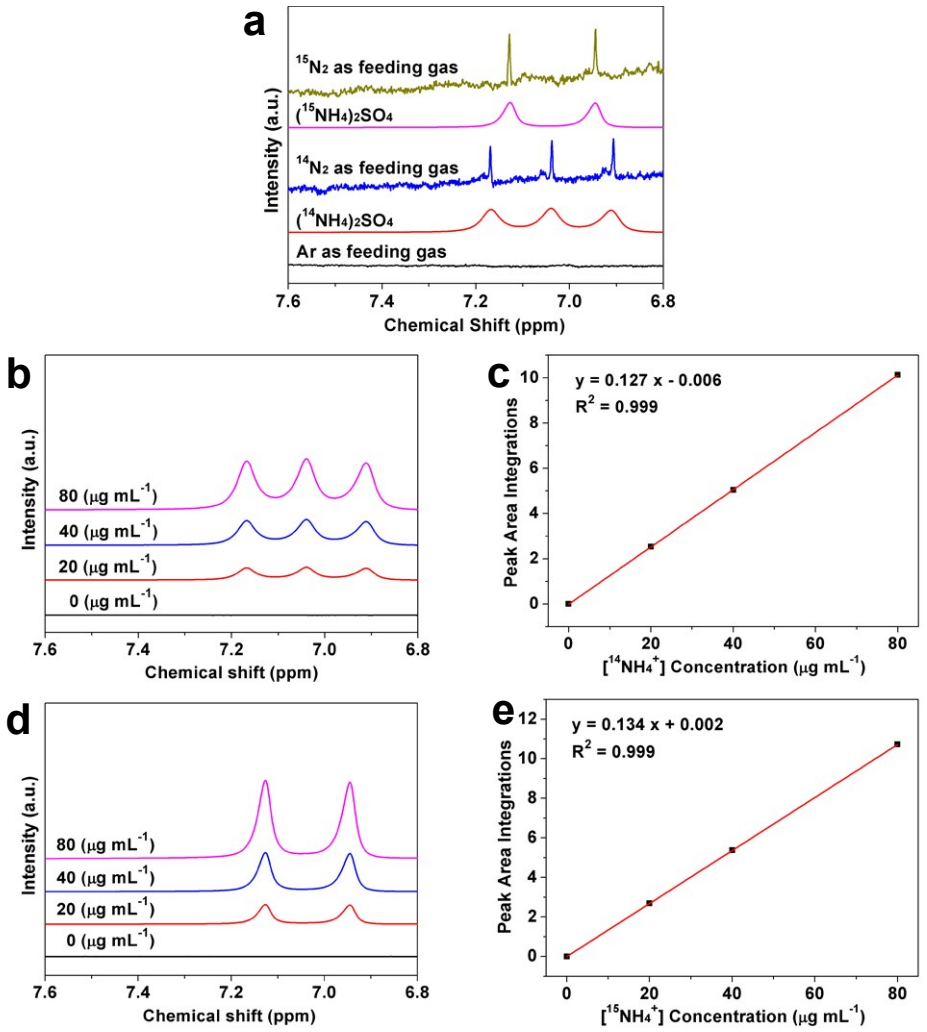

Fig. S16 (a) ^{1}H NMR spectra obtained for the post-electrolysis 0.1 M Na_2SO_4 electrolytes with Ar, $^{14}N_2$ or $^{15}N_2$ as the feeding gas, respectively. $(^{14}NH_4)_2SO_4$ or $(^{15}NH_4)_2SO_4$ dissolved 0.1 M Na_2SO_4 electrolyte was used as the standard solution. (b, d) ^{1}H NMR spectra of the $^{14}NH_4^+$ and $^{15}NH_4^+$ standards with different concentrations. (c, e) Corresponding $^{14}NH_4^+$ and $^{15}NH_4^+$ calibration curves constructed by plotting the integrated ^{1}H NMR peak area against standard concentration.

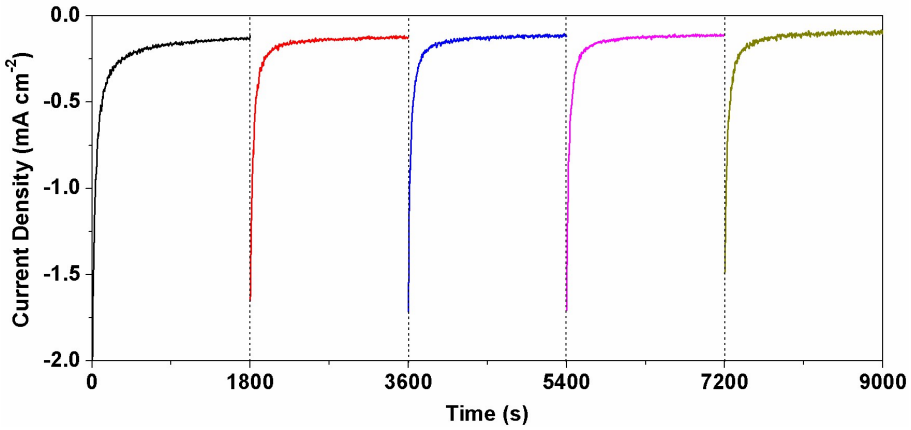

Fig. S17 Recycling stability test of the $Nb_3O_7(OH)$/CFC catalyst in N_2-saturated 0.1 M Na_2SO_4 electrolyte at -0.4 V *vs.* RHE with each recycling experiment of 30 min. After every cycle, the electrolyte was collected for measurement and fresh electrolyte was added to the electrochemical cell for another cycle experiment.

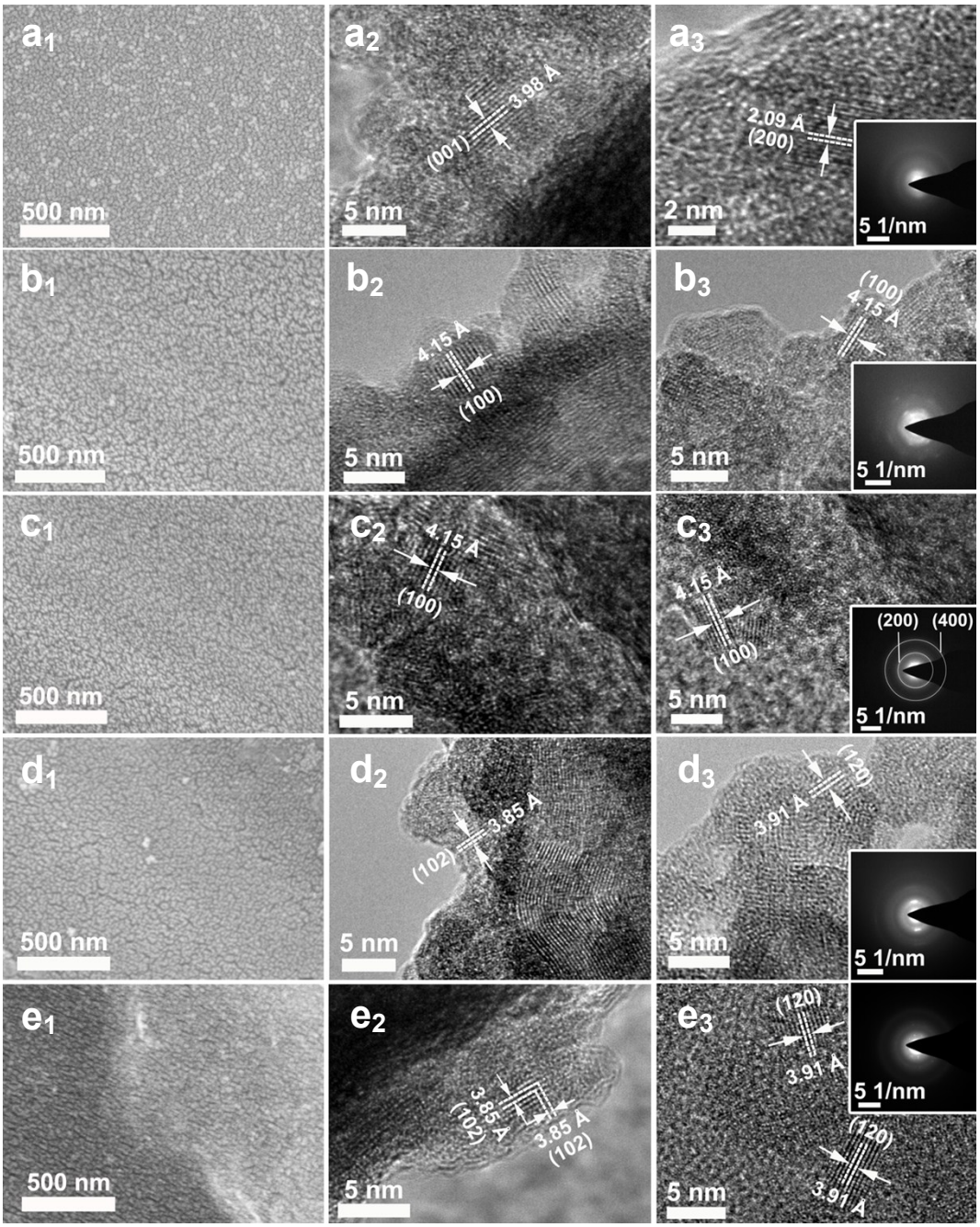

Fig. S18 SEM images (a_1-e_1), HRTEM images (a_2-e_2, a_3-e_3) and corresponding SAED patterns (insets in a_3-e_3) of $Nb_3O_7(OH)$/CFC after NRR at -0.4 V *vs.* RHE for different times. (a_1-a_3) Cat-200 s; (b_1-b_3) Cat-15 min; (c_1-c_3) Cat-30 min; (d_1-d_3) Cat-5 h; (e_1-e_3) Cat-10 h.

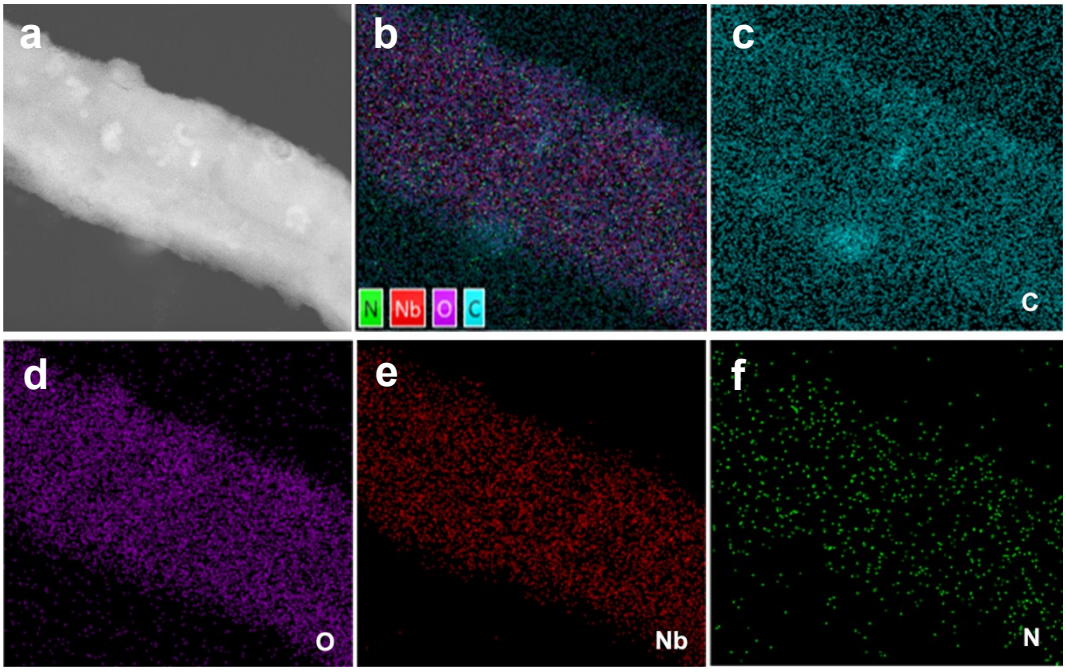

Fig. S19 (a) High-angle annular dark-field scanning transmission electron microscopy (HAADF-STEM) and (b-f) corresponding elemental mapping images of $Nb_3O_7(OH)$/CFC after the long-term durability measurement for 10 h (Cat-10 h).

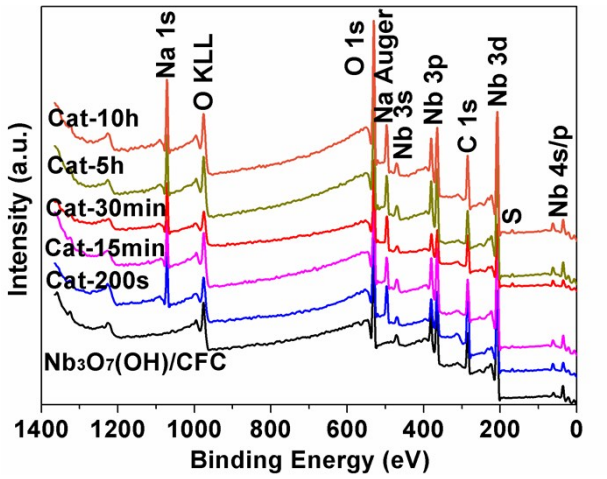

Fig. S20 XPS survey spectra of the $Nb_3O_7(OH)$/CFC after NRR at -0.4 V *vs.* RHE with different reaction time.

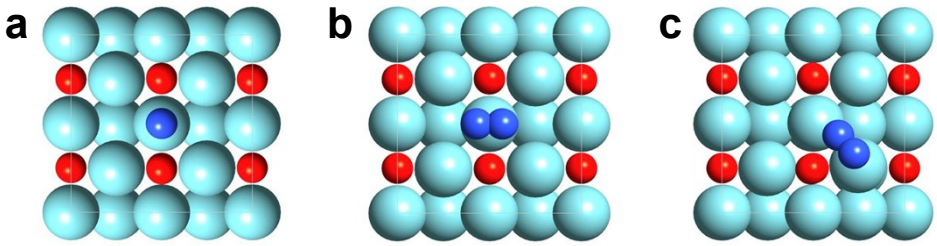

Fig. S21 Top view of relaxed N_2 adsorption configurations. (a) End-on-top; (b) Side-on-top; (c) Side-on-bridge. Sky blue sphere: Nb; red sphere: O; deep blue sphere: N.

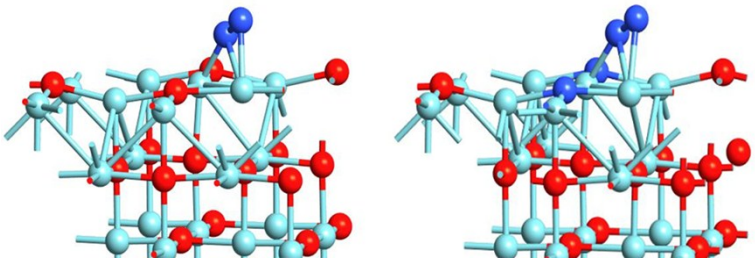

Fig. S22 Optimized geometric structures of $*N_2$ adsorption on NbO (left) and N substituted NbO (right). Sky blue sphere: Nb; red sphere: O; deep blue sphere: N.

References

1. J. Wang, L. Yu, L. Hu, G. Chen, H. Xin and X. Feng, *Nat. Commun.*, 2018, **9**, 1795.
2. M. M. Shi, D. Bao, S. J. Li, B. R. Wulan, J. M. Yan and Q. Jiang, *Adv. Energy Mater.*, 2018, **8**, 1800124.
3. M. Nazemi, S. R. Panikkanvalappil and M. A. El-Sayed, *Nano Energy*, 2018, **49**, 316-323.
4. Q. Qin, T. Heil, M. Antonietti and M. Oschatz, *Small Methods*, 2018, **2**, 1800202.
5. X. Wang, W. Wang, M. Qiao, G. Wu, W. Chen, T. Yuan, Q. Xu, M. Chen, Y. Zhang, X. Wang, J. Wang, J. Ge, X. Hong, Y. Li, Y. Wu and Y. Li, *Sci. Bull.*, 2018, **63**, 1246-1253.
6. Z. Geng, Y. Liu, X. Kong, P. Li, K. Li, Z. Liu, J. Du, M. Shu, R. Si and J. Zeng, *Adv. Mater.*, 2018, **30**, 1803498.
7. H. Tao, C. Choi, L. X. Ding, Z. Jiang, Z. Han, M. Jia, Q. Fan, Y. Gao, H. Wang, A. W. Robertson, S. Hong, Y. Jung, S. Liu and Z. Sun, *Chem*, 2019, **5**, 204-214.
8. Z. Wang, F. Gong, L. Zhang, R. Wang, L. Ji, Q. Liu, Y. Luo, H. Guo, Y. Li, P. Gao, X. Shi, B. Li, B. Tang and X. Sun, *Adv. Sci.*, 2018, 1801182.
9. X. Wu, L. Xia, Y. Wang, W. Lu, Q. Liu, X. Shi and X. Sun, *Small*, 2018, **14**, 1803111.
10. L. Zhang, X. Ji, X. Ren, Y. Ma, X. Shi, Z. Tian, A. M. Asiri, L. Chen, B. Tang and X. Sun, *Adv. Mater.*, 2018, **30**, 1800191.
11. X. Li, T. Li, Y. Ma, Q. Wei, W. Qiu, H. Guo, X. Shi, P. Zhang, A. M. Asiri, L. Chen, B. Tang and X. Sun, *Adv. Energy Mater.*, 2018, **8**, 1801357.
12. K. Jia, Y. Wang, Q. Pan, B. Zhong, Y. Luo, G. Cui, X. Guo and X. Sun, *Nanoscale Adv.*, 2019, **1**, 961-964.
13. L. Yang, T. Wu, R. Zhang, H. Zhou, L. Xia, X. Shi, H. Zheng, Y. Zhang and X. Sun, *Nanoscale*, 2019, **11**, 1555-1562.
14. L. Zhang, X. Ren, Y. Luo, X. Shi, A. M. Asiri, T. Li and X. Sun, *Chem. Commun.*, 2018, **54**, 12966-12969.
15. J. Han, Z. Liu, Y. Ma, G. Cui, F. Xie, F. Wang, Y. Wu, S. Gao, Y. Xu and X. Sun, *Nano Energy*, 2018, **52**, 264-270.

16. W. Kong, Z. Liu, J. Han, L. Xia, Y. Wang, Q. Liu, X. Shi, Y. Wu, Y. Xu and X. Sun, *Inorg. Chem. Front.*, 2019, **6**, 423-427.
17. L. Huang, J. Wu, P. Han, A. M. Al-Enizi, T. M. Almutairi, L. Zhang and G. Zheng, *Small Methods*, 2018, 1800386.
18. H. Du, X. Guo, R. M. Kong and F. Qu, *Chem. Commun.*, 2018, **54**, 12848-12851.
19. H. Cheng, L. X. Ding, G. F. Chen, L. Zhang, J. Xue and H. Wang, *Adv. Mater.*, 2018, **30**, 1803694.
20. B. Xu, L. Xia, F. Zhou, R. Zhao, H. Chen, T. Wang, Q. Zhou, Q. Liu, G. Cui, X. Xiong, F. Gong and X. Sun, *ACS Sustainable Chem. Eng.*, 2019, **7**, 2889-2893.
21. X. Li, L. Li, X. Ren, D. Wu, Y. Zhang, H. Ma, X. Sun, B. Du, Q. Wei and B. Li, *Ind. Eng. Chem. Res.*, 2018, **57**, 16622-16627.
22. L. Xia, X. Wu, Y. Wang, Z. Niu, Q. Liu, T. Li, X. Shi, A. M. Asiri and X. Sun, *Small Methods*, 2018, 1800251.
23. W. Qiu, X. Y. Xie, J. Qiu, W. H. Fang, R. Liang, X. Ren, X. Ji, G. Cui, A. M. Asiri, G. Cui, B. Tang and X. Sun, *Nat. Commun.*, 2018, **9**, 3485.
24. X. Yu, P. Han, Z. Wei, L. Huang, Z. Gu, S. Peng, J. Ma and G. Zheng, *Joule*, 2018, **2**, 1610-1622.
25. L. Zhang, L. X. Ding, G. F. Chen, X. Yang and H. Wang, *Angew. Chem., Int. Ed.*, 2019, **58**, 2612-2616.
26. C. Lv, Y. Qian, C. Yan, Y. Ding, Y. Liu, G. Chen and G. Yu, *Angew. Chem., Int. Ed.*, 2018, **57**, 10246-10250.